Pitavastatin counteracts venetoclax resistance mechanisms in acute myeloid leukemia by depleting geranylgeranyl pyrophosphate

Running title: Pitavastatin overcomes venetoclax resistance in AML

Roberta Buono[1*], Dennis Juarez[1]*, Madhuri Paul[1]*, Sarah J. Skuli[2], Ian B. Wong[1], Ishita Tarnekar[1], Zhili Ying[1], Izabelle Le[3], Gerald Wertheim[2], A'ishah Bakayoko[2], Marisa Kruidenier[2], Said M. Sebti[4], Marina Konopleva[5], Angela G. Fleischman[6], Cholsoon Jang[3], Martin Carroll[2], David A. Fruman[1]. * these authors contributed equally to this work

Affiliations

[1] Department of Molecular Biology & Biochemistry, University of California Irvine, Irvine, CA, 92697, USA; [2] Department of Medicine, Division of Hematology & Oncology, University of Pennsylvania, Philadelphia, PA 19104, USA; [3] Department of Biological Chemistry, Center for Epigenetics and Metabolism, Department of Chemistry, University of California Irvine, Irvine, CA, 92697, USA; [4] Department of Pharmacology and Toxicology and Massey Comprehensive Cancer Center, Virginia Commonwealth University, Richmond, VA, 23298, USA; [5] Albert Einstein Colege of Medicine, Montefiore Einstein Comprehensive Cancer Center, 1300 Morris Park Ave, Bronx, NY, 10461, USA; [6] Division of Hematology-Oncology, Department of Medicine, University of California Irvine, Irvine, CA, 92697, USA.

Address Correspondence:

David A. Fruman, PhD, UC Irvine, 839 Health Sciences Road, 216 Sprague Hall, Irvine, CA, 92697-3905. dfruman@uci.edu

or

Roberta Buono, PhD, UC Irvine, 839 Health Sciences Road, 216 Sprague Hall, Irvine, CA, 92697-3905. buonor@uci.edu

Competing Interests Statement

SMS is co-inventor of GGTI-2418 and GGTI-2417, and is Scientific Founder of Prescient Therapeutics. MK receives research support and serves a consultant and advisory board member for AbbVie. The other authors have no competing interests to disclose.

Abstract

The BCL2 inhibitor venetoclax has therapeutic activity in several hematological malignancies. In acute myeloid leukemia (AML), venetoclax combined with hypomethylating agents is the standard of care for patients unfit for intensive chemotherapy, but intrinsic and acquired resistance are common. Loss of p53 function is strongly associated with venetoclax resistance, and adding venetoclax to 5-azacitidine provides no overall survival benefit in *TP53*-mutant AML. Other frequent mechanisms of venetoclax resistance in AML include *FLT3* mutations, MCL-1 upregulation, and altered mitochondrial metabolism. Unfortunately, it has been challenging to develop agents that target these mechanisms directly and combinatorially. Here we report that pitavastatin, an inhibitor of HMG-CoA-reductase, promotes apoptosis and overcomes several venetoclax resistance mechanisms in human AML cells. At clinically achievable concentrations, pitavastatin treatment has potent cytotoxic activity in cells with mutations in *TP53* or *FLT3*. The apoptotic mechanism involves p53-independent PUMA upregulation and reduced MCL-1 expression. Pitavastatin also suppresses mitochondrial gene expression and oxidative metabolism. The pro-apoptotic actions of pitavastatin depend on depletion of geranylgeranyl pyrophosphate (GGPP) and can be recapitulated by inhibiting GGPP synthase or geranylgeranyltransferase-1 enzymes. These results provide a mechanistic rationale for adding pitavastatin to AML regimens to prevent or overcome venetoclax resistance.

Introduction

B cell lymphoma 2 (BCL2) is an oncoprotein and a member of a family of apoptosis-regulating proteins (1). The pro-survival family members (BCL2, BCL-xL, MCL-1, BCL-w, BFL-1) contain four domains with homology to BCL2 (BH1, BH2, BH3, BH4). Levels of these proteins are often elevated in blood cancer cells to escape stress-induced increases of pro-apoptotic proteins, including "BH3-only" proteins such as BIM and PUMA (1–3). BH3 mimetics are cell-permeable small molecules that block the BH3-binding pocket of BCL2 family members, inhibiting their pro-survival function and promoting apoptosis (1–3). Their clinical utility is validated by BCL2-selective venetoclax (ABT-199) regimens for front-line treatment of chronic lymphocytic leukemia (CLL) and acute myeloid leukemia (AML) (4,5). However, there remains a critical need to identify combinations that further broaden and deepen responses to venetoclax and prevent the emergence of resistance (6).

AML demonstrates diverse resistance mechanisms to BCL2 inhibition. Despite initial success in the treatment of *TP53*-mutant CLL (4), subsequent basic and clinical studies highlight that bi-allelic *TP53* loss is a frequent mechanism of resistance in AML (7–9). Indeed, while venetoclax combined with 5-azacitidine (AZA) extends survival in AML patients unfit for intensive chemotherapy (10), this combination provides no overall survival benefit compared to AZA alone in patients with *TP53* loss (11,12). Other factors associated with venetoclax resistance in AML include reduced mitochondrial priming through upregulation of other anti-apoptotic proteins such as MCL-1 (13), certain genetic drivers (e.g., *FLT3*-internal tandem duplication (ITD) and *RAS*; (8,14)), *BCL2* mutations (15), and altered mitochondrial dynamics including increased respiration (16–19).

The mevalonate pathway is a targetable cancer dependency that supports proliferation and survival (20,21). Many oncogenes increase cellular demand for mevalonate pathway outputs, while driving mevalonate flux by increasing expression of HMG-CoA-reductase (HMGCR) or other pathway enzymes (21). This has spurred interest in repurposing statins (selective HMGCR inhibitors) for oncology (21–24). We reported that statins promote apoptosis and sensitize to venetoclax in blood cancer cell lines and primary cells (25,26), a finding independently validated by others (27,28). Our retrospective analysis of venetoclax clinical trials revealed that statin use is associated with significantly increased rates of complete response in CLL or multiple myeloma (MM) (25,26). These findings provided rationale for a prospective phase 1 clinical trial (clinicaltrials.gov identifier NCT04512105) testing pitavastatin in combination with venetoclax in AML and CLL. This trial found that the addition of pitavastatin to venetoclax regimens is tolerable (29).

Barriers that have limited the clinical translation of statins as oncology drugs include the many mechanisms of action described in the literature and the underappreciated role of statin pharmacology in design of clinical trials (21,30). We previously determined that the pro-apoptotic effect of statins is due to depletion of cellular pools of geranylgeranyl pyrophosphate (GGPP) (25,26), the isoprenoid substrate for protein geranylgeranylation, and this finding is generalizable to several of the described mechanisms of statin's anti-cancer effects (21,31). Concerning statin pharmacology, we found that pitavastatin has approximately 3-fold greater potency than other statins in cell-based assays, and acts at clinically achievable concentrations to block geranylgeranylation and promote apoptosis in MM cells (26). Pitavastatin in our phase I trial also demonstrated preliminary signs of efficacy with all subjects achieving complete remission (29).

Here we assess statin efficacy against AML venetoclax resistance using cell line models and primary cells. To focus on mevalonate pathway outputs relevant to survival signaling in AML cells, we identify cellular responses that are induced by pitavastatin in a manner dependent on GGPP depletion and are recapitulated by geranylgeranyltransferase-1 (GGTase-1) inhibitors. These analyses revealed that pitavastatin sensitizes to venetoclax via p53-independent upregulation of PUMA and by rewiring cellular transcription to disrupt mitochondrial gene expression and metabolism. In a subset of AML cells, pitavastatin diminishes the expression of MCL-1. Together, these results show that pitavastatin can overcome several common mechanisms of venetoclax resistance in AML and should be assessed in combination with venetoclax and AZA in future clinical trials.

Materials and Methods

Additional Methods provided in the supplement.

Cell Culture

AML cell lines (Table 1) were obtained from commercial repositories (ATCC or DSMZ) and authenticated annually through STR profiling using the University of Arizona Genomics Core. MOLM13 parental and venetoclax resistant were described previously (32). Cell lines were tested for mycoplasma infection annually. Unless otherwise noted, cell lines used in the study were maintained in RPMI-1640, 10% FBS, 1% penicillin-streptomycin-glutamine (Gibco) and 10 mM HEPES (Corning).

Human cells were provided by UCI biobank or U-Penn (Table 2) and cultured in IMDM supplemented with 15% BIT 9500 with and 1 μM StemRegenin 1 (Stemcells Technologies), plus

human cytokines (Peprotech): SCF (100 ng/ml), Flt3-Ligand (50 ng/ml), IL-3 (20 ng/ml), G-CSF (20 ng/ml), 1:100 penicillin-streptomycin-glutamine, and 50 μM beta mercaptoethanol.

Statistics and experimental design

Statistical analysis was performed in Prism10 using one-way or two-way ANOVA, as appropriate for each experiment and indicated in the legends. Post-tests for multiple comparisons were recommended by Prism and applied as noted in the Figure legends. All samples represent biological replicates. Unless otherwise specified in figure legends, all center values shown in graphs refer to the mean. The number of biological replicates (n) and details of the tests are provided in the figure legends. $p < 0.05$ was considered statistically significant and was annotated throughout as * $p < 0.05$, ** $p < 0.01$, *** $p < 0.001$ and **** $p < 0.001$.

Results

Pitavastatin induces p53-independent cytotoxicity at sub-micromolar concentrations in AML cells

Previously we reported that simvastatin sensitizes AML cell lines to venetoclax cytotoxicity (25), and that pitavastatin is cytotoxic in MM cell lines at lower concentrations than simvastatin (26). Here we tested pitavastatin in a panel of AML cell lines with different genetic lesions (Table 1). Cytotoxicity assays demonstrated that 48-hour treatment with pitavastatin concentrations as low as 300 nM reduced viability in OCI-AML3 and HNT-34 cells and enhanced the weak cytotoxic effect of venetoclax (Figure 1A). A similar effect was observed in MV4-11 cells at 1 μM pitavastatin (Figure 1A). The mechanism by which pitavastatin enhanced

113 cytotoxicity was caspase-dependent, as it was blocked by the inhibitor Q-VD-OPh at 24hr (Fig.
114 S1A). In the MOLM13 and PL-21 cell lines, pitavastatin alone had minimal cytotoxic activity
115 but enhanced the effect of venetoclax (Figure 1A). Pitavastatin retained cytotoxicity in a
116 venetoclax-resistant subline of MOLM13 (32) (Fig. S1B). The combination of pitavastatin and
117 venetoclax was synergistic in OCI-AML3, HNT-34, MV4-11, and MOLM13 cells (Table S1; the
118 latter three cell lines have *FLT*3-ITD). We identified a pitavastatin-resistant AML cell line (OCI-
119 M1) (Figure 1A, Table S1) that we used as a comparator for mechanistic studies. Consistent with
120 prior publications (25), simvastatin enhanced venetoclax cytotoxicity but only at concentrations
121 above 1 μM in OCI-AML3 and MOLM13 cells (Fig. S1C).
122 We extended these studies to cultures of primary AML cells obtained from cryopreserved adult
123 AML mononuclear specimens (Table 2). Primary cultures were more pitavastatin sensitive than
124 established cell lines with notable cytotoxicity at 100 – 300 nM including three samples with
125 *TP53* mutations and three out of five samples with *FLT3*-ITD (Figure 1B and S2A, B, C).
126 Venetoclax further enhanced the killing of several of the primary AML samples (Figure 1B). In
127 addition, pitavastatin increased cytotoxicity of the combination of venetoclax and AZA in several
128 primary AML samples (Fig. S2C). In most of these samples, the combination of venetoclax plus
129 pitavastatin was more effective than venetoclax plus AZA.
130 We showed previously that expression of a dominant-negative p53 did not affect simvastatin-
131 mediated cytotoxicity or venetoclax sensitization in OCI-AML3 cells (25). To investigate further
132 the relationship of p53 status to pitavastatin sensitivity, we used isogenic MOLM14 cell lines
133 with either wild-type or bi-allelic deletion of *TP53*, generated by CRISPR/Cas9 (33). In parental
134 MOLM14 cells, pitavastatin in the 1-3 μM concentration range was sufficient to promote cell
135 death (Fig. S3). The p53-deficient MOLM14 variants, which are resistant to cytarabine (33) and

136 less sensitive than control MOLM14 cells to venetoclax (Fig. S3), remained sensitive to
137 pitavastatin and to the synergistic or additive cytotoxicity of pitavastatin plus venetoclax (Fig.
138 S3, Table S2).
139 Overall, the findings that pitavastatin at submicromolar concentrations (clinically achievable
140 with FDA-approved doses, enhances the cytotoxic activity of venetoclax in a variety of AML cell
141 lines and primary cells, and that primary AML cells are more sensitive to pitavastatin at lower
142 concentrations than AML cell lines, suggest that addition of pitavastatin to venetoclax regimens
143 in AML may be a feasible approach for treatment, including in cases with p53 inactivation or
144 *FLT3*-ITD.
145
146 *Pitavastatin alters expression of BCL2 family members PUMA and MCL-1*
147 p53-independent upregulation of PUMA is a general mechanism by which statins sensitize
148 blood cancer cells to BH3 mimetics (25,26). Consistent with our previous findings, pitavastatin
149 treatment increased expression of PUMA protein in OCI-AML3, HNT-34 and MV4-11 cell lines
150 that are sensitive to statin cytotoxicity (Fig. S4A, B, C). Pitavastatin treatment caused lesser or
151 no PUMA upregulation in cell lines that are less sensitive (MOLM-13, PL-21) or resistant to
152 cytotoxicity (OCI-M1) (Fig. S4A, B, D). Additionally, in isogenic *TP53* deleted MOLM14 cells,
153 pitavastatin induced PUMA expression to a comparable degree in control (Fig. S5A).
154 CRISPR/Cas9-mediated knockout of the *BBC3* gene encoding PUMA (Fig. S5B, C) partially
155 reversed the cytotoxic effect of pitavastatin in OCI-AML3 and MOLM-14 cells but not in
156 MOLM-13 cells (Figure 2A).
157 Increased expression of and dependence on MCL-1 can confer venetoclax resistance in AML
158 cells (34,35). We assessed how venetoclax and pitavastatin co-treatment affects protein

159 expression of PUMA and MCL1. In OCI-AML3, MOLM13, and MOLM14 cells, pitavastatin
160 reduced expression of MCL-1 and/or prevented the increase in MCL-1 following venetoclax
161 treatment (Fig. S6A, B). In general, the combination of pitavastatin with venetoclax reduced
162 MCL-1 expression more than pitavastatin alone. We also noted that in some AML cell lines,
163 venetoclax reduced PUMA expression and suppressed PUMA upregulation by pitavastatin (Fig.
164 S6A, B). In the venetoclax-resistant MOLM13 subline, pitavastatin increased low basal PUMA
165 expression but did not reduce the high basal MCL-1 expression (Fig. S6C). In two of the three
166 *TP53* mutant primary AML cells we tested, 24hr treatment with pitavastatin reduced MCL-1 or
167 increased PUMA expression (Fig. S6D). Thus, pitavastatin can alter the balance of pro- and anti-
168 apoptotic BCL2 family members via at least two mechanisms.
169
170 *Pitavastatin increases cytotoxicity and PUMA expression via depletion of GGPP and inhibition*
171 *of geranylgeranylation*
172 In most blood cancer cell models, statin cytotoxicity is linked to depletion of isoprenoid
173 intermediates downstream of mevalonate (36,37). Using an antibody that detects the
174 unprenylated form of RAP1A GTPase, we found that pitavastatin inhibited geranylgeranylation
175 at 1 μM or lower concentrations in all cell lines except OCI-M1 (Figure 2B, D and S4C, D). In
176 addition, supplementing culture medium with excess GGPP prevented pitavastatin-induced
177 PUMA expression (Figure 2B, C) and cytotoxicity (Fig. S7A) in statin-sensitive cells. This result
178 suggests that GGPP depletion is required for the pitavastatin mechanism of action. To determine
179 whether GGPP-depletion is sufficient, we used an inhibitor of GGPP synthase (THZ145; (38))
180 and found that it had cytotoxic activity in OCI-AML3 cells and increased PUMA expression to a
181 similar extent as pitavastatin (Fig. S7B, C).

We showed previously that a GGTase-I inhibitor, GGTI-298, increased PUMA in AML cells (25). Unexpectedly, while GGTI-298 upregulated PUMA, had cytotoxic activity, and sensitized to venetoclax, the structurally related GGTI-2133 had minimal effects on these functional readouts (Figures 2D, E and S7B, C). GGTI-2133 had equivalent or greater ability to reduce prenylation of RAP1A, a commonly used readout of GGTase-1 activity (Figure 2D and S7B). Furthermore, both compounds reduced actin polymerization, which is driven by GTPases such as RHO, RAC and CDC42 known to be substrates of GGTase-1 (21,31) (Fig. S8A). Thus, GGTI-2133 and GGTI-298 both have observed activity on inhibition of GGTase-I substrates, yet GGTI-298 more closely phenocopies the anti-cancer effects of pitavastatin on AML cell function. It is unlikely that the effects of GGTI-298 are simply due to off-target activity on farnesyltransferases or other enzymes, given that GGPP synthase inhibition had cytotoxic activity similar to statins. Moreover, a more selective and potent GGTase-1 inhibitor (GGTI-2417; (39)) exerted cytotoxic activity in AML cell lines and increased PUMA expression and unprenylated RAP1A (Fig. S8B-D). Together these data support the conclusion that GGTase-1 is a key prenyltransferase mediating pro-survival activities of GGPP in AML cell lines.

Pitavastatin and GGTI-298 elicit widespread transcriptome changes including enhanced apoptotic gene signatures

A challenge to applying transcriptome studies to decipher statin cytotoxic mechanism is that there are multiple outputs of the mevalonate pathway, of which only some play key roles in cell survival regulation. We reasoned that differentially expressed genes (DEGs) shared in pitavastatin and GGTI-298 treatment conditions but not after GGTI-2133 treatment are most relevant to the cytotoxic mechanism. In accord, we treated OCI-AML3 and HNT-34 cells with

205 vehicle alone (0.1% DMSO) or pitavastatin (PIT; 1 μM) or GGTIs (10 μM) and harvested RNA
206 for bulk RNA sequencing. We chose a time point (16hr) before the onset of apoptosis but when
207 PUMA upregulation is observed at the protein level.
208 Pitavastatin and GGTI-298 each caused broad changes in gene expression (vs. vehicle
209 condition, Supplementary Excel File 1) with a high degree of overlap in both OCI-AML3
210 (Figure 3A) and HNT-34 (Fig. S9A). GGTI-2133 treatment altered expression of many fewer
211 genes in both cell lines (Figure 3A and S9A, Supplementary Excel File 1). Principal component
212 analysis (PCA) supported the similarity of cells treated with GGTI-2133 or vehicle alone (Fig.
213 S9B). In accord, unbiased transcriptome-wide analysis of rlog-based sample distances
214 demonstrated clustering of vehicle with GGTI-2133 and of PIT with GGTI-298 in both OCI-
215 AML3 and HNT-34 (Fig. S9C). Gene set enrichment analysis (GSEA) for Hallmark and
216 Reactome pathways in OCI-AML3 cells showed several shared responses to pitavastatin and
217 GGTI-298, including reduced expression of MYC and E2F targets and an increase in genes
218 associated with apoptosis (Figure 3B). Similar gene sets were identified in HNT-34 cells, which
219 also displayed a signature of cholesterol homeostasis and SREBP targets suggesting a stronger
220 feedback response (Figure 3B). The *SREBF2* mRNA was increased by both pitavastatin and
221 GGTI-298, but not GGTI-2133, with a greater effect in HNT-34 cells (Fig. S10). In agreement
222 with the increase PUMA protein expression, the *BBC3* gene encoding PUMA was significantly
223 upregulated by pitavastatin and GGTI-298, but not GGTI-2133, in both cell lines (Fig. S10).
224
225 *Transcriptome analysis of pitavastatin effects dependent on GGPP depletion*
226 As a second approach to defining statin cytotoxic mechanism, we determined which gene
227 expression changes induced by pitavastatin are dependent on GGPP depletion. We conducted

228 RNA sequencing on OCI-AML3 cells treated for 16hr with vehicle alone, pitavastatin, GGPP or
229 PIT + GGPP. Compared to vehicle-treated samples, there were ~1400 DEGs in the PIT-treated
230 condition but only 129 in the GGPP condition and 103 in the PIT+GGPP condition (Figure 4A).
231 Applying a $\log_2$ fold-change (LFC) cut-off of +/- 0.1, there were only three DEGs in the
232 PIT+GGPP vs. Vehicle condition and one in the GGPP vs. Vehicle (Supplementary Excel File 2).
233 PCA showed that PIT-treated samples clustered together and distant from the other three groups
234 (Fig. S11A). These data indicate that statin-mediated transcriptional reprogramming at 16hr is
235 almost entirely dependent on GGPP depletion. In MOLM13 cells, which are less pitavastatin
236 sensitive than OCI-AML3 cells (Figure 1), pitavastatin caused many fewer DEGs yet these were
237 still largely dependent on GGPP depletion (add S11B). Hallmark GSEA analysis of OCI-AML3
238 cells showed downregulation of MYC and E2F targets (Figure 4B), consistent with the first
239 transcriptome experiment.
240 An independent approach using Ingenuity Pathway Analysis software also identified
241 MYC/E2F downregulation and PUMA upregulation, along with c-JUN upregulation, as cellular
242 mechanisms induced by pitavastatin and GGTI-298 (Fig. S9D).
243
244 *Functional validation of transcription factor targets*
245 To investigate the mechanism of reduced MYC target gene expression, we measured changes
246 in MYC protein by western blot. Treatment of OCI-AML3 cells with pitavastatin reduced MYC
247 expression, an effect that was reversed by mevalonate or GGPP and phenocopied by GGTI-298
248 and GGTI-2417, but not GGTI-2133 (Figure 5A, B; S12). Pitavastatin also reduced MYC protein
249 amounts in primary AML samples UCI-01 and UCI-06 (Figure 5A). MYC protein
250 downregulation was not observed in PL-21 cells (resistant to pitavastatin single-agent

251 cytotoxicity) but was also minimal in HNT-34 cells (sensitive to pitavastatin cytotoxicity)
252 (Figure 5A, B).
253 Downregulation of MYC and E2F is commonly observed under conditions of cell cycle
254 arrest (40,41). Accordingly, we found that pitavastatin and GGTI-298, but not GGTI-2133,
255 increased the proportion of cells in G1 and decreased S phase in OCI-AML3 cells (Figure 5C).
256 Pitavastatin and GGTI-298 had minimal effects on cell cycle in HNT-34 cells (Figure 5C) in
257 alignment with the preservation of MYC protein expression (Figure 5A).
258 Pitavastatin strongly increased expression of the *TSC22D3* gene, with similar induction by
259 GGTI-298 but to a lesser extent by GGTI-2133 (Fig. S10). *TSC22D3* encodes the glucocorticoid-
260 induced leucine zipper (GILZ) protein that contributes to dexamethasone-induced apoptosis in
261 MM cells (42). In accord with mRNA changes, protein measurements by western blot showed
262 that pitavastatin increased GILZ expression in statin-sensitive cell lines but not in resistant PL-21
263 cells (Figure 5A, B). Addition of GGPP prevented the pitavastatin-induced GILZ expression
264 (Fig. S13A). However, CRISPR/Cas9-mediated deletion of GILZ in OCI-AML3 cells did not
265 affect cell viability changes in response to pitavastatin alone or the combination with venetoclax
266 (Fig. S13B, C). These data suggest that GILZ induction is not essential for statin cytotoxicity.
267
268 *Pitavastatin suppresses oxidative metabolism and TCA cycle in OCI-AML3 cells*
269 GSEA analysis showed that pitavastatin and/or GGTI-298 reduced gene sets associated with
270 mitochondrial protein import and oxidative phosphorylation (Figure 3C, 4B). Combined analysis
271 of data from OCI-AML3 cells in both transcriptome studies identified a set of 85 shared DEGs
272 representing nuclear-encoded mitochondrial genes, of which only 3 were significantly changed
273 by GGTI-2133 (Fig. 6A). A large majority of these were downregulated, including genes whose

274 products regulate the function of components of the electronic transport chain (*CYCS*, *DHODH*,
275 *NDUFAF4*, *TIMM21*, *TMEM126B*, *TMEM177*). The smaller subset of upregulated mitochondrial
276 genes included *BBC3* (Figure 6A).

277 The changes in expression of mRNAs encoding mitochondrial proteins prompted us to assess
278 mitochondrial mass and function. Pitavastatin reduced expression of the mitochondrial protein
279 TOM20 in OCI-AML3 cells but not MOLM13 cells (Fig. S14A); however, only one of two
280 alternate assays for mitochondrial mass gave similar results (Fig. S14B, C). Seahorse metabolic
281 flux analysis showed that pitavastatin reduced basal oxygen consumption rate (OCR) in OCI-
282 AML3 cells but not in MOLM13 cells (Figure 6B, C), consistent with the lack of downregulation
283 of mitochondrial genes in MOLM13. Addition of GGPP partially reversed the decreased basal
284 OCR in OCI-AML3 cells treated with pitavastatin (Figure 6D). The combination of pitavastatin
285 with venetoclax strongly and significantly reduced basal OCR and spare respiratory capacity in
286 OCI-AML3 and MOLM13 cells (Fig. S15A, B). However, after 16hr of treatment with
287 venetoclax +/- pitavastatin, a large percentage of cells had released cytochrome C (Fig. S15C,
288 D), effects that might indirectly suppress OCR. Cytochrome C release did not occur with
289 pitavastatin alone (Fig. S15C), a condition where basal OCR was reduced in OCI-AML3 cells
290 (Figure 6B, C). Concurrent with decreased OCR, pitavastatin also caused loss of mitochondrial
291 membrane potential in a significant percentage of OCI-AML3, as well as MOLM14 parental and
292 *TP53* mutant lines (Fig. S16A, B).

293 To investigate whether mitochondrial dysfunction is associated with metabolic flux, we
294 conducted untargeted metabolomics combined with [U-^{13}C]-glucose tracing. The data revealed
295 that, in OCI-AML3 cells, 16-hour pitavastatin treatment significantly reduced the production of
296 TCA cycle intermediates from glucose (Figure 6E).

297

298 **Discussion**

299 The combination of venetoclax with 5-azacitidine (VEN-AZA) is a standard of care regimen
300 for AML patients who are >75 years old or unfit for intensive chemotherapy. As first-line therapy
301 in previously untreated AML patients, VEN-AZA increases the frequency of complete remission
302 and provides an increase in median OS compared to AZA alone (10). However, it has become
303 clear that VEN-AZA provides no survival advantage compared to AZA alone in the subgroup
304 with *TP53* loss of function (11,12). In addition, venetoclax resistance is common in AML cases
305 with *FLT3*-ITD and/or *RAS* mutations, enhanced mitochondrial metabolism, or MCL-1
306 overexpression (8,13,14,18). Currently there are no clinically used drugs that can address
307 multiple venetoclax resistance mechanisms. Here we show that an FDA-approved HMGCR
308 inhibitor, pitavastatin, potentiates venetoclax cytotoxicity in multiple AML cell models including
309 established and primary AML cells with *TP53* mutations or *FLT3*-ITD. In most statin-sensitive
310 cell lines, pitavastatin upregulates the pro-apoptotic protein PUMA. In some cell lines,
311 pitavastatin decreases MCL-1, and can inhibit oxidative metabolism.

312 The selective cytotoxicity of statins in AML compared to normal hematopoietic progenitors
313 was first reported more than 30 years ago (43). Why has this not yet led to application in clinical
314 practice? Three reasons deserve prominent attention. First, the great majority of cell-based assays
315 in the literature employ concentrations of statins (5-20 μM) that are 100 – 1000 times higher than
316 clinical achievable by the statin drugs most prescribed (i.e., simvastatin, atorvastatin,
317 rosuvastatin). Thus, the cytotoxic effects and mechanisms described *in vitro* have questionable
318 relevance to the clinical scenario. Second, it is essential to choose hydrophobic statin drugs with
319 good bioavailability (30). Some prospective AML clinical trials have used hydrophilic statins

320 (e.g., pravastatin; (44,45)) that, even at high doses, do not readily enter blood cells that lack
321 active transport mechanisms. Third, statin pharmacology is different in rodents (46), resulting in
322 inadequate inhibition of the mevalonate pathway and generally weak *in vivo* anti-cancer effects
323 in preclinical models (33,47), which can diminish enthusiasm for advancing to human trials.
324 Pitavastatin has gained recognition as an ideal molecule for applications in oncology (30).
325 This compound is ~3-times more potent on a molar basis in cell lines, achieves plasma
326 concentrations in the 200 – 500 nM range in humans at the FDA-approved dose, and has an
327 extended half-life and fewer drug interactions than other statins (21,26,48,49). Our phase 1
328 clinical trial found that daily 2 or 4 mg doses of pitavastatin were well tolerated in AML and
329 CLL patients receiving venetoclax as standard of care (29). In this study, we show that
330 pitavastatin is more potent than simvastatin in AML cell lines. While the concentration of
331 pitavastatin that has single-agent cytotoxicity varies among AML cell lines from 0.3 to 3 μM, we
332 observe activity in primary AML cells at concentrations in the 0.1 – 0.3 μM range. Importantly,
333 pitavastatin is active in *TP53*-mutant samples regardless of their sensitivity to VEN or AZA.
334 Pitavastatin enhanced venetoclax cytotoxicity in four AML cell lines with FLT3-ITD (MOLM13,
335 MOLM14, MV4.11, PL-21) and in three out of five primary samples tested (UCI-03, -07, -09).
336 Selective inhibition of BCL2 with venetoclax is most effective in cancers that depend on
337 BCL2 for survival. Basal or acquired dependence on MCL-1 is a common mechanism of
338 venetoclax resistance in AML (34,50,51). Unfortunately, direct targeting of MCL-1 with highly
339 selective compounds is associated with significant adverse events (52). Suppressing MCL-1
340 transcription via CDK9 inhibitors is another strategy under investigation (53). Pitavastatin is an
341 alternative option, based on our observation that the compound can overcome venetoclax-
342 induced increases in MCL-1 expression. In these experiments, we observed that in several AML

343 cell lines, treatment with venetoclax or the combination of pitavastatin with venetoclax reduced
344 PUMA protein amounts compared to basal. Thus, the mechanisms of cytotoxicity may differ in
345 response to pitavastatin alone versus the combination with venetoclax.
346 There has been considerable interest in targeting oxidative metabolism to treat AML.
347 Preclinical studies established that AML cell venetoclax resistance correlates with increased
348 mitochondrial metabolism (17,18,54). Furthermore, various OXPHOS inhibitors potentiate
349 cytotoxicity of venetoclax and prevent or overcome resistance (17,18,55,56). A selective
350 inhibitor of complex-1 of the electron transport chain entered clinical trials but a phase I study
351 reported significant toxicities and lack of efficacy at tolerated doses (57,58). Treatment with
352 pitavastatin might provide an alternative, well-tolerated route to achieve a reduction in
353 mitochondrial respiration. Our data show that at a time point before the onset of apoptosis,
354 pitavastatin reduces basal OCR while triggering MMP loss in a significant fraction of cells. In
355 OCI-AML3 cells, these mitochondrial defects were accompanied by decreased flux of glucose to
356 the TCA cycle. In a separate paper, we reported that pitavastatin and rosuvastatin reverse the
357 increase in OXPHOS observed in cytarabine-resistant *TP53*-mutant AML cells (33).
358 Mitochondrial dysfunction has the potential to reduce ATP production and cause activation of
359 AMPK, a pathway that can promote PUMA expression via the integrated stress response (ISR) in
360 AML cells (54). We previously showed that pitavastatin activates the ISR in MM cell lines;
361 however, under the same conditions a chemical inhibitor of the ISR did not affect statin
362 cytotoxicity or venetoclax sensitization in AML cell lines (26).
363 The effects of pitavastatin on AML cell survival, PUMA upregulation, and OXPHOS are
364 dependent on GGPP depletion as they are largely rescued by exogenous GGPP. Furthermore, two
365 inhibitors of GGTase-1 recapitulated many actions of pitavastatin, supporting the hypothesis that

366 GGTase-1 substrates have essential functions in AML cell survival. A key question is how the
367 mevalonate/GGPP axis programs AML transcription to promote proliferation and survival. To
368 address this, we determined which transcriptional changes induced by pitavastatin are
369 recapitulated by GGTI-298 and reversed by GGPP. Together these transcriptome analyses
370 revealed several novel findings. First, the mevalonate pathway via GGPP promotes expression of
371 cMYC and E2F target genes, correlating with cell cycle progression. Second, the mevalonate
372 pathway regulates expression of many nuclear-encoded mitochondrial genes, some which are
373 associated with OXPHOS. This connection might underly how treatment with pitavastatin
374 reduces basal OCR and spare respiratory capacity and disrupts MMP. Notably, the extent of
375 pitavastatin-induced transcriptional reprogramming is quite variable, with more prominent
376 effects in OCI-AML3 cells compared to other lines tested here (Supplementary Excel files with
377 volcano plots). This might be due in part to varying levels of positive feedback reactivation of
378 the mevalonate pathway (59); indeed, pitavastatin-treated HNT-34 cells had a strong cholesterol
379 pathway upregulation signature and overall fewer DEGs than OCI-AML3 cells. It is possible that
380 the kinetics of transcriptional reprogramming differs among cell lines such that a shared DEG
381 signature is difficult to define. Ongoing work aims to (i) identify transcription factors or
382 epigenetic changes underlying altered gene expression and (ii) determine which
383 geranylgeranylated protiens transmit key survival signals that are disrupted by statin treatment.
384 To broaden the utility of venetoclax in AML, it is essential to identify new combination
385 regimens that address common mechanisms of resistance. In this study we have presented
386 evidence that pitavastatin, an FDA-approved agent, has potent cytotoxic activity in human AML
387 cells including samples with *TP53* loss. Pitavastatin treatment achieves several cellular changes
388 that sensitize to venetoclax including PUMA upregulation, MCL-1 downregulation, and reduced

respiration. Together with other findings from various laboratories (27,28,30), these results support further investigation of pitavastatin/venetoclax combinations in AML.

Acknowledgements

The authors thank Dr. Elizabeth Brèm and Dr. Joel Leverson for helpful discussions. We acknowledge and appreciate research contributions from undergraduate students Nilufar Montazer, Ashley Navarro, Bita Sadrossadat, Jennifer Ly, Harrison Unger, and Enoc Ulloa. This work was supported by the UC Irvine Training Program for Interdisciplinary Cancer Research (T32-CA009054, to DJ), the UPenn Hematology Clinical Research Training Program (T32-HL0439, to SJS), research grants from the National Institutes of Health (R01-AA029124 to CJ; U54CA283759, to MC), an Impact Award from the Department of Defense Peer-Reviewed Cancer Research Program (W81XWH-20-1-0867, to DAF), a Veterans Merit Award (I01BX000918, to MC), a Discovery Boost grant from the American Cancer Society (DBG-24-1319247, to DAF), a Pew Scholar Award (to CJ), the American Society of Hematology (to SJS), American Society of Clinical Oncology (to SJS), and by an Anti-Cancer Challenge pilot grant (to DAF) from the Chao Family Comprehensive Cancer Center (supported by P30-CA062203). The project used Shared Resources of the Chao Family Comprehensive Cancer Center (Optical Biology Core; Biostatistics Shared Resource; Experimental Tissue Resource).

Author Contributions

Supervision: RB, DJ, MP, SJS, CJ, MC, DAF. Funding acquisition: SJS, SMS, CJ, MC, DAF. Conceptualization: RB, DJ, MP, SJS, MC, DAF. Methodology/Provision of models/reagents: SJS, GW, SMS, MK, AGF, CJ, MC. Data collection: RB, DJ, MP, SJS, IBW, IT, ZY, IL, AB, MK. Data analysis and interpretation: RB, DJ, MP, SJS, IBW, IT, ZY, IL, CJ, MC, DAF. Bioinformatics: RB, DJ, MP. Statistical analysis: RB, DJ, MP, SJS. Figure preparation: RB. Writing – original draft: RB, DJ, MP, DAF. Critical review of the manuscript & writing – review and editing prior to finalization: All authors.

Data Availability

RNA-seq datasets produced in this study will be available in the GEO databases (deposit is in progress).

References

1. Cory S, Roberts AW, Colman PM, Adams JM. Targeting BCL-2-like Proteins to Kill Cancer Cells. Trends Cancer. 2016 Aug;2(8):443–60.
2. Leverson JD, Sampath D, Souers AJ, Rosenberg SH, Fairbrother WJ, Amiot M, et al. Found in Translation: How Preclinical Research Is Guiding the Clinical Development of the BCL2-Selective Inhibitor Venetoclax. Cancer Discov. 2017 Dec;7(12):1376–93.
3. Merino D, Kelly GL, Lessene G, Wei AH, Roberts AW, Strasser A. BH3-Mimetic Drugs: Blazing the Trail for New Cancer Medicines. Cancer Cell. 2018 Dec 10;34(6):879–91.
4. Roberts AW, Davids MS, Pagel JM, Kahl BS, Puvvada SD, Gerecitano JF, et al. Targeting BCL2 with Venetoclax in Relapsed Chronic Lymphocytic Leukemia. N Engl J Med. 2016 Jan 28;374(4):311–22.
5. DiNardo CD, Pratz K, Pullarkat V, Jonas BA, Arellano M, Becker PS, et al. Venetoclax combined with decitabine or azacitidine in treatment-naive, elderly patients with acute myeloid leukemia. Blood. 2019 Jan 3;133(1):7–17.
6. Grant S. Rational combination strategies to enhance venetoclax activity and overcome resistance in hematologic malignancies. Leuk Lymphoma. 2017 Aug 24;59(6):1–8.
7. Nechiporuk T, Kurtz SE, Nikolova O, Liu T, Jones CL, D'Alessandro A, et al. The TP53 apoptotic network is a primary mediator of resistance to BCL2 inhibition in AML cells. Cancer Discov. 2019 Jul;9(7):910–25.
8. DiNardo CD, Tiong IS, Quaglieri A, MacRaild S, Loghavi S, Brown FC, et al. Molecular patterns of response and treatment failure after frontline venetoclax combinations in older patients with AML. Blood. 2020 Mar 12;135(11):791–803.

449 9. Thijssen R, Diepstraten ST, Moujalled D, Chew E, Flensburg C, Shi MX, et al. Intact TP-
450 53 function is essential for sustaining durable responses to BH3-mimetic drugs in
451 leukemias. Blood. 2021 May 20;137(20):2721–35.
452 10. DiNardo CD, Jonas BA, Pullarkat V, Thirman MJ, Garcia JS, Wei AH, et al. Azacitidine
453 and venetoclax in previously untreated acute myeloid leukemia. N Engl J Med. 2020 Aug
454 13;383(7):617–29.
455 11. Pollyea DA, Pratz KW, Wei AH, Pullarkat V, Jonas BA, Recher C, et al. Outcomes in
456 Patients with Poor-Risk Cytogenetics with or without TP53 Mutations Treated with
457 Venetoclax and Azacitidine. Clin Cancer Res. 2022 Dec 15;28(24):5272–9.
458 12. Döhner H, Pratz KW, DiNardo CD, Wei AH, Jonas BA, Pullarkat VA, et al. Genetic risk
459 stratification and outcomes among treatment-naive patients with AML treated with
460 venetoclax and azacitidine. Blood. 2024 Nov 21;144(21):2211–22.
461 13. Bhatt S, Pioso MS, Olesinski EA, Yilma B, Ryan JA, Mashaka T, et al. Reduced
462 mitochondrial apoptotic priming drives resistance to BH3 mimetics in acute myeloid
463 leukemia. Cancer Cell. 2020 Dec 14;38(6):872-890.e6.
464 14. Sango J, Carcamo S, Sirenko M, Maiti A, Mansour H, Ulukaya G, et al. RAS-mutant
465 leukaemia stem cells drive clinical resistance to venetoclax. Nature. 2024
466 Dec;636(8041):241–50.
467 15. Brown FC, Wang X, Birkinshaw R, Chua CC, Morley T, Kasapgil S, et al. Acquired
468 BCL2 variants associated with venetoclax resistance in acute myeloid leukemia. Blood
469 Adv. 2025 Jan 14;9(1):127–31.

470 16. Sharon D, Cathelin S, Mirali S, Di Trani JM, Yanofsky DJ, Keon KA, et al. Inhibition of
471 mitochondrial translation overcomes venetoclax resistance in AML through activation of
472 the integrated stress response. Sci Transl Med. 2019 Oct 30;11(516).
473 17. Liu F, Kalpage HA, Wang D, Edwards H, Hüttemann M, Ma J, et al. Cotargeting of
474 Mitochondrial Complex I and Bcl-2 Shows Antileukemic Activity against Acute Myeloid
475 Leukemia Cells Reliant on Oxidative Phosphorylation. Cancers (Basel). 2020 Aug
476 24;12(9).
477 18. Bosc C, Saland E, Bousard A, Gadaud N, Sabatier M, Cognet G, et al. Mitochondrial
478 inhibitors circumvent adaptive resistance to venetoclax and cytarabine combination
479 therapy in acute myeloid leukemia. Nat Cancer. 2021 Nov 11;2(11):1204–23.
480 19. Glytsou C, Chen X, Zacharioudakis E, Al-Santli W, Zhou H, Nadorp B, et al. Mitophagy
481 promotes resistance to BH3 mimetics in acute myeloid leukemia. Cancer Discov. 2023
482 Jul 7;13(7):1656–77.
483 20. Mullen PJ, Yu R, Longo J, Archer MC, Penn LZ. The interplay between cell signalling
484 and the mevalonate pathway in cancer. Nat Rev Cancer. 2016 Nov;16(11):718–31.
485 21. Juarez D, Fruman DA. Targeting the mevalonate pathway in cancer. Trends Cancer. 2021
486 Jun;7(6):525–40.
487 22. Clendening JW, Penn LZ. Targeting tumor cell metabolism with statins. Oncogene. 2012
488 Nov 29;31(48):4967–78.
489 23. Longo J, van Leeuwen JE, Elbaz M, Branchard E, Penn LZ. Statins as anticancer agents
490 in the era of precision medicine. Clin Cancer Res. 2020 Nov 15;26(22):5791–800.
491 24. Tripathi S, Gupta E, Galande S. Statins as anti-tumor agents: A paradigm for repurposed
492 drugs. Cancer Rep (Hoboken). 2024 May;7(5):e2078.

493 25. Lee JS, Roberts A, Juarez D, Vo T-TT, Bhatt S, Herzog L-O, et al. Statins enhance
494 efficacy of venetoclax in blood cancers. Sci Transl Med. 2018 Jun 13;10(445).
495 26. Juarez D, Buono R, Matulis SM, Gupta VA, Duong M, Yudiono J, et al. Statin-induced
496 Mitochondrial Priming Sensitizes Multiple Myeloma Cells to BCL2 and MCL-1
497 Inhibitors. Cancer Res Commun. 2023 Dec 8;3(12):2497–509.
498 27. Gimenez N, Tripathi R, Giró A, Rosich L, López-Guerra M, López-Oreja I, et al. Systems
499 biology drug screening identifies statins as enhancers of current therapies in chronic
500 lymphocytic leukemia. Sci Rep. 2020 Dec 17;10(1):22153.
501 28. Al-Zebeeby A, Vogler M, Milani M, Richards C, Alotibi A, Greaves G, et al. Targeting
502 intermediary metabolism enhances the efficacy of BH3 mimetic therapy in hematologic
503 malignancies. Haematologica. 2019;104(5):1016–25.
504 29. Brem EA, Shieh K, Juarez D, Buono R, Jeyakumar D, O'Brien S, et al. A phase 1 study
505 of adding pitavastatin to venetoclax-based therapy in AML and CLL/SLL: a tolerable,
506 mechanism-based, drug repurposing strategy. Blood Neoplasia. 2024 Aug;100036.
507 30. Abdullah MI, de Wolf E, Jawad MJ, Richardson A. The poor design of clinical trials of
508 statins in oncology may explain their failure - Lessons for drug repurposing. Cancer Treat
509 Rev. 2018 Sep;69:84–9.
510 31. Wang M, Casey PJ. Protein prenylation: unique fats make their mark on biology. Nat Rev
511 Mol Cell Biol. 2016 Feb;17(2):110–22.
512 32. Han L, Zhang Q, Dail M, Shi C, Cavazos A, Ruvolo VR, et al. Concomitant targeting of
513 BCL2 with venetoclax and MAPK signaling with cobimetinib in acute myeloid leukemia
514 models. Haematologica. 2020 Mar;105(3):697–707.

515 33. Skuli SJ, Bakayoko A, Kruidenier M, Manning B, Pammer P, Salimov A, et al.
516 Chemoresistance of TP53 mutant acute myeloid leukemia requires the mevalonate
517 byproduct, geranylgeranyl pyrophosphate, for induction of an adaptive stress response.
518 Leukemia. 2025 Jul 9;39:2087–2098.
519 34. Teh TC, Nguyen N-Y, Moujalled DM, Segal D, Pomilio G, Rijal S, et al. Enhancing
520 venetoclax activity in acute myeloid leukemia by co-targeting MCL1. Leukemia. 2017 Jul
521 28;32(2):303–12.
522 35. Caenepeel S, Brown SP, Belmontes B, Moody G, Keegan KS, Chui D, et al. AMG 176, a
523 Selective MCL1 Inhibitor, Is Effective in Hematologic Cancer Models Alone and in
524 Combination with Established Therapies. Cancer Discov. 2018 Dec;8(12):1582–97.
525 36. Xia Z, Tan MM, Wong WW, Dimitroulakos J, Minden MD, Penn LZ. Blocking protein
526 geranylgeranylation is essential for lovastatin-induced apoptosis of human acute myeloid
527 leukemia cells. Leukemia. 2001 Sep;15(9):1398–407.
528 37. Wong WW-L, Clendening JW, Martirosyan A, Boutros PC, Bros C, Khosravi F, et al.
529 Determinants of sensitivity to lovastatin-induced apoptosis in multiple myeloma. Mol
530 Cancer Ther. 2007 Jun;6(6):1886–97.
531 38. Xia Y, Xie Y, Yu Z, Xiao H, Jiang G, Zhou X, et al. The mevalonate pathway is a
532 druggable target for vaccine adjuvant discovery. Cell. 2018 Nov 1;175(4):1059-1073.e21.
533 39. Peng H, Carrico D, Thai V, Blaskovich M, Bucher C, Pusateri EE, et al. Synthesis and
534 evaluation of potent, highly-selective, 3-aryl-piperazinone inhibitors of protein
535 geranylgeranyltransferase-I. Org Biomol Chem. 2006 May 7;4(9):1768–84.
536 40. Schuldiner O, Benvenisty N. A DNA microarray screen for genes involved in c-MYC and
537 N-MYC oncogenesis in human tumors. Oncogene. 2001 Aug 16;20(36):4984–94.

538 41. Baudino TA, Maclean KH, Brennan J, Parganas E, Yang C, Aslanian A, et al. Myc-
539 mediated proliferation and lymphomagenesis, but not apoptosis, are compromised by
540 E2f1 loss. Mol Cell. 2003 Apr;11(4):905–14.
541 42. Kervoëlen C, Ménoret E, Gomez-Bougie P, Bataille R, Godon C, Marionneau-Lambot S,
542 et al. Dexamethasone-induced cell death is restricted to specific molecular subgroups of
543 multiple myeloma. Oncotarget. 2015 Sep 29;6(29):26922–34.
544 43. Newman A, Clutterbuck RD, Powles RL, Millar JL. Selective inhibition of primary acute
545 myeloid leukaemia cell growth by simvastatin. Leukemia. 1994 Nov;8(11):2023–9.
546 44. Kornblau SM, Banker DE, Stirewalt D, Shen D, Lemker E, Verstovsek S, et al. Blockade
547 of adaptive defensive changes in cholesterol uptake and synthesis in AML by the addition
548 of pravastatin to idarubicin + high-dose Ara-C: a phase 1 study. Blood. 2007 Apr
549 1;109(7):2999–3006.
550 45. Advani AS, Li H, Michaelis LC, Medeiros BC, Liedtke M, List AF, et al. Report of the
551 relapsed/refractory cohort of SWOG S0919: A phase 2 study of idarubicin and cytarabine
552 in combination with pravastatin for acute myelogenous leukemia (AML). Leuk Res. 2018
553 Apr;67:17–20.
554 46. Schonewille M, de Boer JF, Mele L, Wolters H, Bloks VW, Wolters JC, et al. Statins
555 increase hepatic cholesterol synthesis and stimulate fecal cholesterol elimination in mice.
556 J Lipid Res. 2016 Aug;57(8):1455–64.
557 47. Hillis AL, Martin TD, Manchester HE, Högström J, Zhang N, Lecky E, et al. Targeting
558 Cholesterol Biosynthesis with Statins Synergizes with AKT Inhibitors in Triple-Negative
559 Breast Cancer. Cancer Res. 2024 Oct 1;84(19):3250–66.

560 48. Catapano AL. Pitavastatin - pharmacological profile from early phase studies. Atheroscler
561 Suppl. 2010 Dec;11(3):3–7.
562 49. Catapano AL. Pitavastatin: a different pharmacological profile. Clin Lipidol. 2012
563 Jun;7(3s):3–9.
564 50. Moujalled DM, Pomilio G, Ghiurau C, Ivey A, Salmon J, Rijal S, et al. Combining BH3-
565 mimetics to target both BCL-2 and MCL1 has potent activity in pre-clinical models of
566 acute myeloid leukemia. Leukemia. 2019;33(4):905–17.
567 51. Zhang Q, Riley-Gillis B, Han L, Jia Y, Lodi A, Zhang H, et al. Activation of RAS/MAPK
568 pathway confers MCL-1 mediated acquired resistance to BCL-2 inhibitor venetoclax in
569 acute myeloid leukemia. Signal Transduct Target Ther. 2022 Feb 21;7(1):51.
570 52. Desai P, Lonial S, Cashen A, Kamdar M, Flinn I, O'Brien S, et al. A Phase 1 First-in-
571 Human Study of the MCL-1 Inhibitor AZD5991 in Patients with Relapsed/Refractory
572 Hematologic Malignancies. Clin Cancer Res. 2024 Nov 1;30(21):4844–55.
573 53. Davids MS, Brander DM, Alvarado-Valero Y, Diefenbach CS, Egan DN, Dinner SN, et
574 al. A phase 1 study of the CDK9 inhibitor voruciclib in relapsed/refractory acute myeloid
575 leukemia and B-cell malignancies. Blood Adv. 2025 Feb 25;9(4):820–32.
576 54. Grenier A, Poulain L, Mondesir J, Jacquel A, Bosc C, Stuani L, et al. AMPK-PERK axis
577 represses oxidative metabolism and enhances apoptotic priming of mitochondria in acute
578 myeloid leukemia. Cell Rep. 2022 Jan 4;38(1):110197.
579 55. Hua L, Yang N, Li Y, Huang K, Jiang X, Liu F, et al. Metformin sensitizes AML cells to
580 venetoclax through endoplasmic reticulum stress-CHOP pathway. Br J Haematol. 2023
581 Jul 6;202(5):971–84.

56. Velez J, Pan R, Lee JTC, Enciso L, Suarez M, Duque JE, et al. Biguanides sensitize leukemia cells to ABT-737-induced apoptosis by inhibiting mitochondrial electron transport. Oncotarget. 2016 Jun 6;7(32):51435–49.

57. Molina JR, Sun Y, Protopopova M, Gera S, Bandi M, Bristow C, et al. An inhibitor of oxidative phosphorylation exploits cancer vulnerability. Nat Med. 2018 Jul;24(7):1036–46.

58. Yap TA, Daver N, Mahendra M, Zhang J, Kamiya-Matsuoka C, Meric-Bernstam F, et al. Complex I inhibitor of oxidative phosphorylation in advanced solid tumors and acute myeloid leukemia: phase I trials. Nat Med. 2023 Jan 19;29(1):115–26.

59. Pandyra A, Mullen PJ, Kalkat M, Yu R, Pong JT, Li Z, et al. Immediate utility of two approved agents to target both the metabolic mevalonate pathway and its restorative feedback loop. Cancer Res. 2014 Sep 1;74(17):4772–82.

Figure Legends

Figure 1: Pitavastatin has potent cytotoxicity in venetoclax-resistant AML cell lines and in patient-derived AML cells. (A) AML cell lines were treated for 48hr with various concentrations of venetoclax alone or with pitavastatin (PIT) at 0.3, 1 and 3 µM. Data are expressed as mean +/- SEM *$p < 0.05$, ****$p < 0.0001$. Two-way ANOVA with Tukey's post hoc test. (B) Patient-derived AML myeloblasts cultured in media with supportive cytokines were treated for 48hr with titrated concentrations of PIT and venetoclax as indicated. For both panels the percentage of viable cells was determined by flow cytometry using Annexin V and PI staining. Identified genetic lesions are shown in parentheses – note three *TP53* mutant samples on the bottom row were all pitavastatin-sensitive.

Figure 2: PUMA upregulation contributes to pitavastatin cytotoxicity, is dependent on GGPP depletion, and is recapitulated by inhibition of GGTase-1. (A) The cytotoxic effect of pitavastatin +/- 30nM venetoclax was measured in two clones of OCI-AML3 cells with PUMA knockout and one clone each of MOLM14 and MOLM13. Two-way ANOVA with Tukey's post hoc test, $n = 3$. (B) PUMA expression in a statin-sensitive AML cell line (OCI-AML3) was assessed by western blot. An antibody to vinculin was used as a loading control. Detection of unprenylated RAP1A was used to determine which treatments suppress protein geranylgeranylation. Note rescue of PIT effect on PUMA by mevalonate (MEV) and GGPP more than by FPP. (C) Quantitation of four replicates of the experiment in panel B, with PUMA expression in vehicle (Veh) treated cells set at 1. Data are expressed as mean +/- SEM ** $p < 0.01$, ***$p < 0.001$, one-way ANOVA with Tukey's post hoc test, $n = 2$-4. (D-E) Different GGTase-1 inhibitors have distinct effects on PUMA expression and viability. (D) Representative

western blot of PUMA expression in OCI-AML3 and MOLM13 treated with pitavastatin (0.3 or 1 μM), GGTI298 (10 μM) or GGTI2133 (10 μM).

(E) Graphs showing percentage of viable OCI-AML3 and MOLM13 measured by Annexin V and PI staining after 48h of treatment with pitavastatin (1 μM+, GGTI298 (10 μM) or GGTI2133 (10 μM) in combination with venetoclax. Data are expressed as mean +/- SEM ***$p < 0.001$, ****$p < 0.0001$. Two-way ANOVA with Tukey's post hoc test, $n \geq 3$.

Figure 3: Transcriptome analysis identifies shared features of the response to PIT and GGTI-298. (A) DEGs in OCI-AML3 cells treated with PIT, GGTI-298, or GGTI-2133, relative to vehicle, were identified by DESeq2, and DEG overlaps were depicted by Venn diagrams and summarized with UpSet plots. (B) GSEA for hallmark and reactome pathways shared by treatment with PIT or GGTI-298. Red indicates GSEA pathways that are upregulated, blue downregulated. Outlined dots are pathways shared in both OCI-AML3 and HNT-34, including downregulation of MYC and E2F targets, and aerobic respiration. The diameter of each dot corresponds to gene set size.

Figure 4: Transcriptome analysis identifies features of the response to PIT that depend on GGPP depletion. (A) Venn diagram and intersection plot showing DEGs in OCI-AML3 cells treated with PIT, GGPP, or PIT + GGPP, compared to vehicle. Note that in the presence of exogenous GGPP, PIT treatment induced very few gene expression changes. (B) GSEA for hallmark (left, including MYC and E2F targets) and reactome pathways (right, including mitochondrial protein import). The p value decreases from blue to red colors, and the diameter of each dot corresponds to gene set size.

Figure 5: Pitavastatin treatment downregulates cMYC expression and increases PUMA and GILZ in AML cell lines and primary cells. (A) Two PIT-sensitive cell lines, one PIT-resistant cell line, and two PIT-sensitive primary AML samples were treated for 16hr as indicated and lysates subjected to western blotting with antibodies to cMYC, PUMA, GILZ, unprenylated RAP1A, and total ERK. (B) Graph of quantitation of western blots from 3-4 experiments for cell lines in panel A, or single experiment for two primary cell samples UCI-01 and UCI-06. Data are expressed as mean +/- SEM *$p < 0.05$, ***$p < 0.001$, ****$p < 0.0001$ two-way ANOVA with Dunnett's test. (C) PIT and GGTI-298 cause G1 arrest in OCI-AML3 cells that are statin sensitive and show consistent MYC downregulation, but not in HNT-34 cells where MYC downregulation is less prominent. Data are expressed as mean +/- SEM *$p < 0.05$, ** $p < 0.01$, ****$p < 0.0001$ two-way ANOVA with Tukey's test, n = 3.

Figure 6: Functional assays provide evidence that PIT causes mitochondrial dysfunction. (A) Heat map of nuclear-encoded mitochondrial genes (MitoCarta database) across conditions in both transcriptome experiments. (B-D) Oxygen consumption rate (OCR) was measured by Seahorse metabolic flux analyzer. (B) Representative Seahorse assay traces in OCI-AML3 and MOLM13 cells treated with vehicle or pitavastatin for 16hr. (C) Graphs depict results of experiments as in panel B, shown as mean +/- SEM, **** $p < 0.0001$ two-way ANOVA with Sidak's test, n = 8. (D) Effect of pitavastatin on basal OCR is significantly reversed by GGPP. * $p < 0.05$, **** $p < 0.0001$ two-way ANOVA with Fisher's least squares difference test, n = 5. (E) ^{13}C-glucose tracing identifies reduced TCA cycle intermediates in OCI-AML3 cells treated with pitavastatin for 16hr (13C-glucose added for last 2hr). Left graph shows quantitation of

glycolytic metabolites, lactate, and acetyl-CoA, containing all ^{13}C atoms traced. Right graph shows TCA cycle metabolites with ^{13}C in M+2 position. Each dot plot depicts results of 3 biological replicates, each representing 4-6 technical replicates, normalized as a ratio of the pitavastatin-treated sample to the vehicle-treated group. * $p < 0.05$, ** $p < 0.01$, *** $p < 0.001$ two-way ANOVA with Fisher's least squares difference test (^ $p = 0.051$ for lactate as marked).

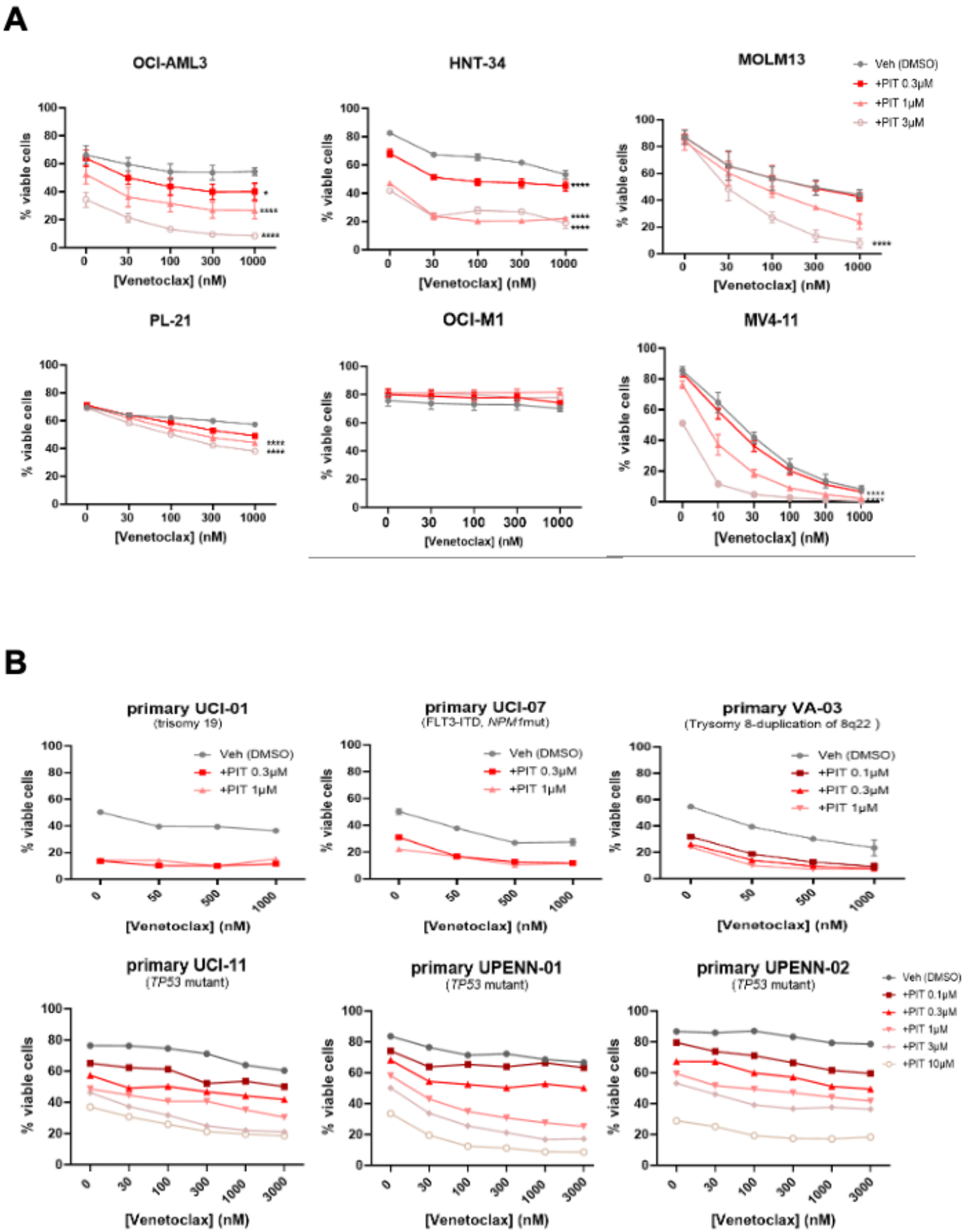
A
OCI-AML3
HNT-34
MOLM13
PL-21
OCI-M1
MV4-11
Veh (DMSO)
+PIT 0.3μM
+PIT 1μM
+PIT 3μM
% viable cells
[Venetoclax] (nM)
B
primary UCI-01
(trisomy 19)
primary UCI-07
(FLT3-ITD, NPM1mut)
primary VA-03
(Trysomy 8-duplication of 8q22)
+PIT 0.1μM
primary UCI-11
(TP53 mutant)
primary UPENN-01
(TP53 mutant)
primary UPENN-02
(TP53 mutant)
+PIT 10μM

Figure 1

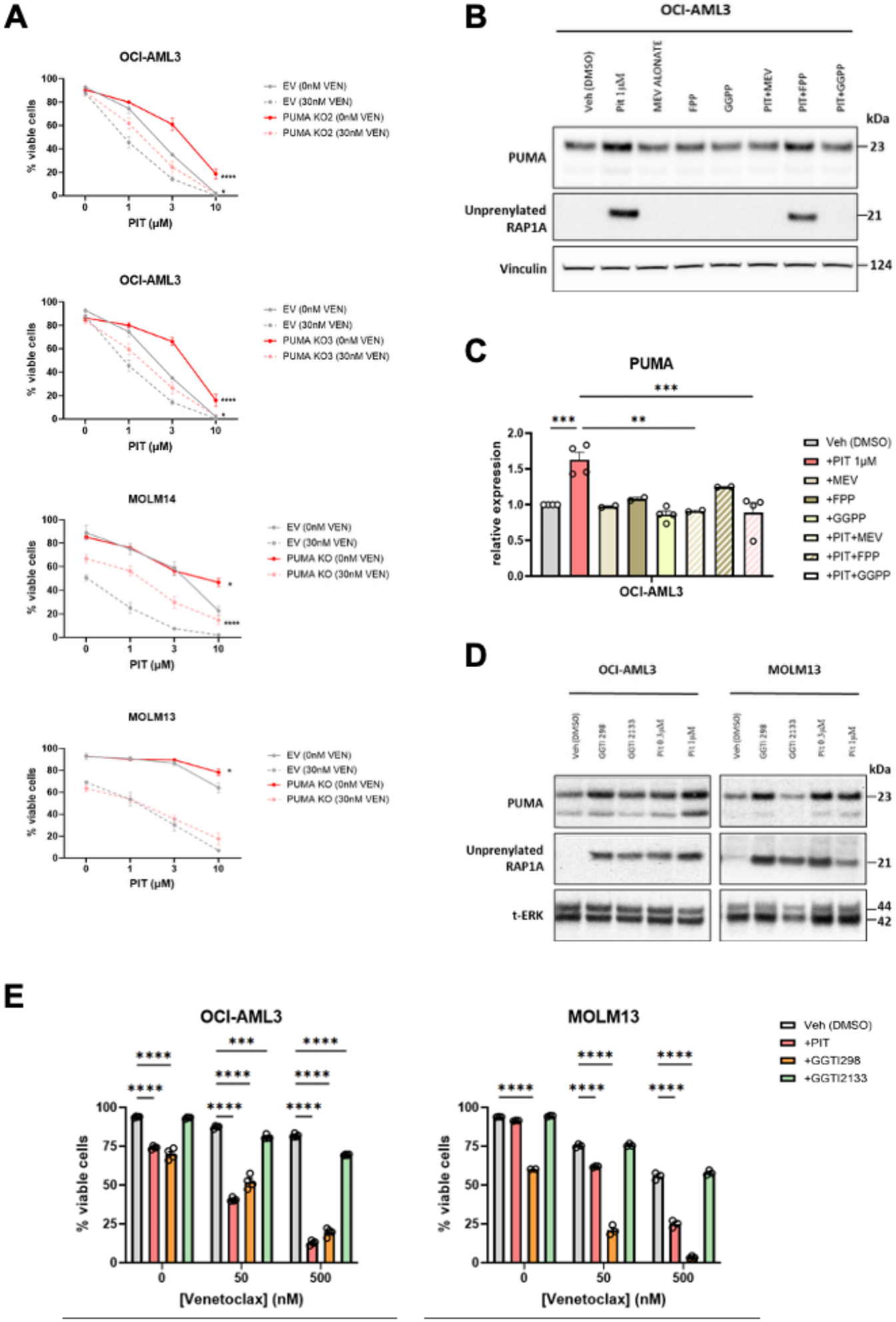
A
OCI-AML3
% viable cells
PIT (μM)
EV (0nM VEN)
EV (30nM VEN)
PUMA KO2 (0nM VEN)
PUMA KO2 (30nM VEN)
OCI-AML3
PUMA KO3 (0nM VEN)
PUMA KO3 (30nM VEN)
MOLM14
PUMA KO (0nM VEN)
PUMA KO (30nM VEN)
MOLM13
B
OCI-AML3
Veh (DMSO)
Pit 1μM
MEV ALONATE
FPP
GGPP
PIT+MEV
PIT+FPP
PIT+GGPP
kDa
PUMA
Unprenylated RAP1A
Vinculin
23
21
124
C
PUMA
relative expression
OCI-AML3
Veh (DMSO)
+PIT 1μM
+MEV
+FPP
+GGPP
+PIT+MEV
+PIT+FPP
+PIT+GGPP
D
OCI-AML3
MOLM13
PUMA
Unprenylated RAP1A
t-ERK
44
42
E
OCI-AML3
MOLM13
% viable cells
[Venetoclax] (nM)
Veh (DMSO)
+PIT
+GGTI298
+GGTI2133

Figure 2

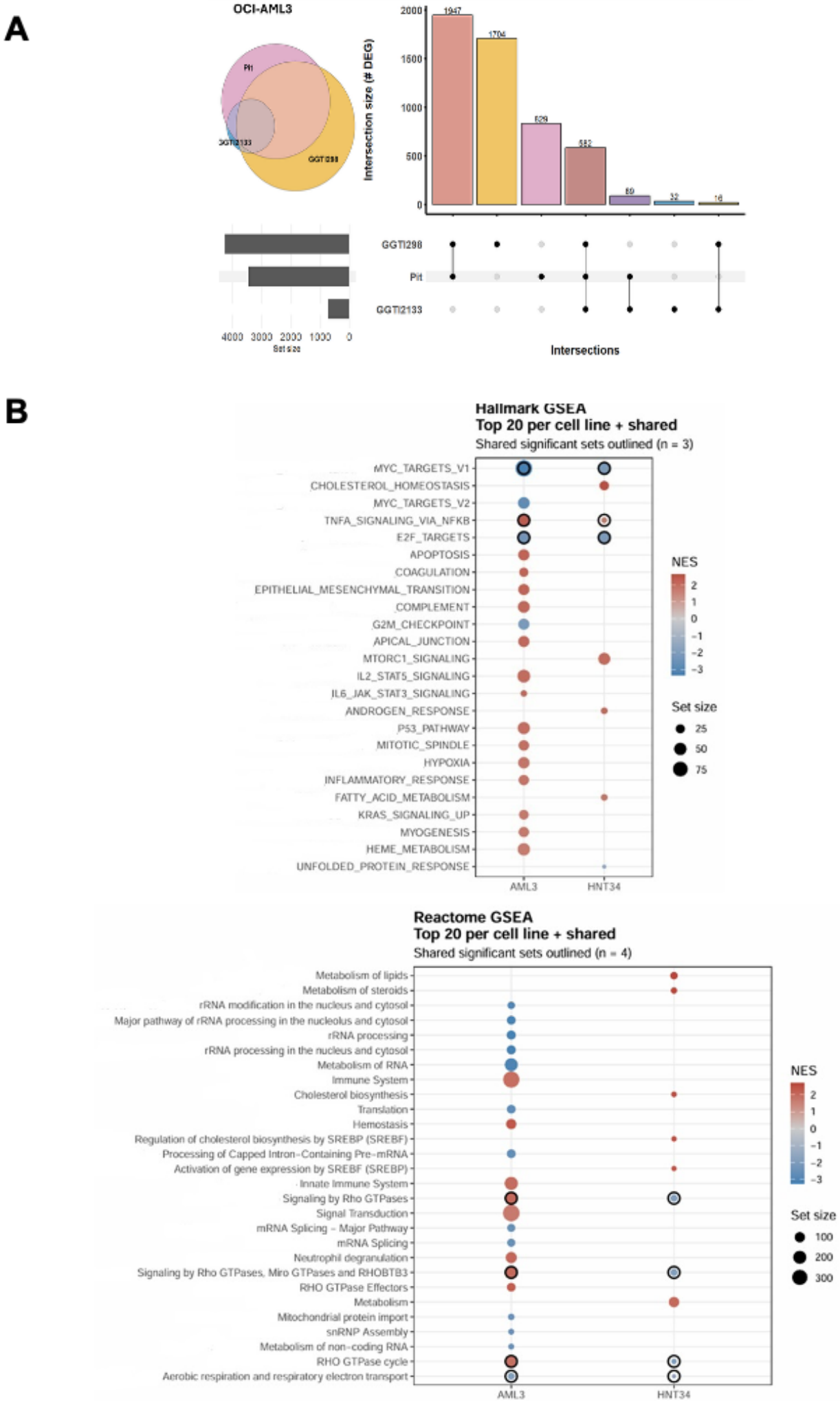
A
OCI-AML3
Pit
GGTI298
GGTI2133
Intersection size (# DEG)
2000
1500
1000
500
0
1947
1704
628
582
89
32
18
GGTI298
Pit
GGTI2133
4000 3000 2000 1000 0
Set size
Intersections
B
Hallmark GSEA
Top 20 per cell line + shared
Shared significant sets outlined (n = 3)
MYC_TARGETS_V1
CHOLESTEROL_HOMEOSTASIS
MYC_TARGETS_V2
TNFA_SIGNALING_VIA_NFKB
E2F_TARGETS
APOPTOSIS
COAGULATION
EPITHELIAL_MESENCHYMAL_TRANSITION
COMPLEMENT
G2M_CHECKPOINT
APICAL_JUNCTION
MTORC1_SIGNALING
IL2_STAT5_SIGNALING
IL6_JAK_STAT3_SIGNALING
ANDROGEN_RESPONSE
P53_PATHWAY
MITOTIC_SPINDLE
HYPOXIA
INFLAMMATORY_RESPONSE
FATTY_ACID_METABOLISM
KRAS_SIGNALING_UP
MYOGENESIS
HEME_METABOLISM
UNFOLDED_PROTEIN_RESPONSE
AML3
HNT34
NES
2
1
0
−1
−2
−3
Set size
25
50
75
Reactome GSEA
Top 20 per cell line + shared
Shared significant sets outlined (n = 4)
Metabolism of lipids
Metabolism of steroids
rRNA modification in the nucleus and cytosol
Major pathway of rRNA processing in the nucleolus and cytosol
rRNA processing
rRNA processing in the nucleus and cytosol
Metabolism of RNA
Immune System
Cholesterol biosynthesis
Translation
Hemostasis
Regulation of cholesterol biosynthesis by SREBP (SREBF)
Processing of Capped Intron-Containing Pre-mRNA
Activation of gene expression by SREBF (SREBP)
Innate Immune System
Signaling by Rho GTPases
Signal Transduction
mRNA Splicing - Major Pathway
mRNA Splicing
Neutrophil degranulation
Signaling by Rho GTPases, Miro GTPases and RHOBTB3
RHO GTPase Effectors
Metabolism
Mitochondrial protein import
snRNP Assembly
Metabolism of non-coding RNA
RHO GTPase cycle
Aerobic respiration and respiratory electron transport
AML3
HNT34
NES
2
1
0
−1
−2
−3
Set size
100
200
300

Figure 3

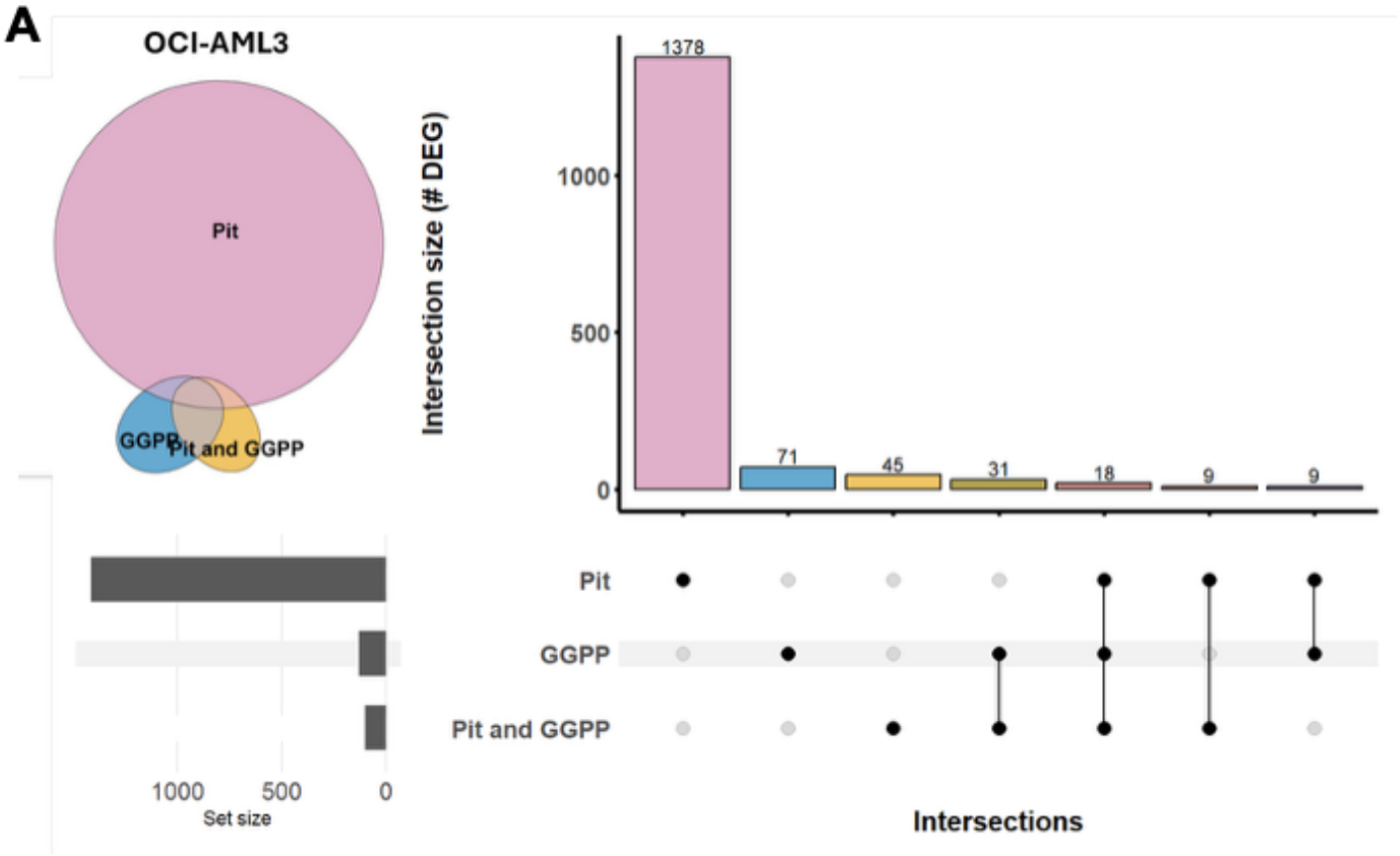
A
OCI-AML3
Pit
GGPP
Pit and GGPP
Intersection size (# DEG)
1378
71
45
31
18
9
9
1000
500
0
Pit
GGPP
Pit and GGPP
1000
500
0
Set size
Intersections

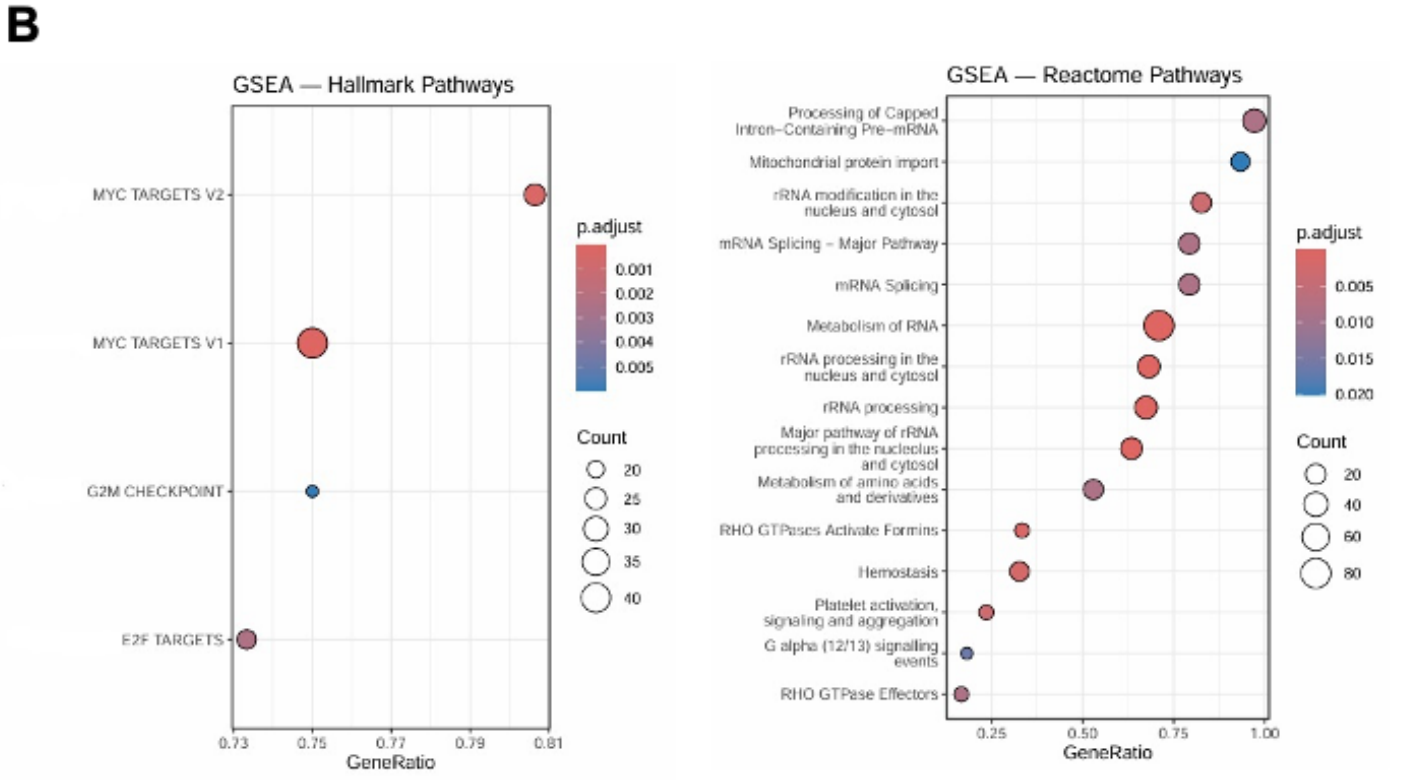
B
GSEA — Hallmark Pathways
MYC TARGETS V2
MYC TARGETS V1
G2M CHECKPOINT
E2F TARGETS
0.73
0.75
0.77
0.79
0.81
GeneRatio
p.adjust
0.001
0.002
0.003
0.004
0.005
Count
20
25
30
35
40
GSEA — Reactome Pathways
Processing of Capped Intron-Containing Pre-mRNA
Mitochondrial protein import
rRNA modification in the nucleus and cytosol
mRNA Splicing - Major Pathway
mRNA Splicing
Metabolism of RNA
rRNA processing in the nucleus and cytosol
rRNA processing
Major pathway of rRNA processing in the nucleolus and cytosol
Metabolism of amino acids and derivatives
RHO GTPases Activate Formins
Hemostasis
Platelet activation, signaling and aggregation
G alpha (12/13) signalling events
RHO GTPase Effectors
0.25
0.50
0.75
1.00
GeneRatio
p.adjust
0.005
0.010
0.015
0.020
Count
20
40
60
80

Figure 4

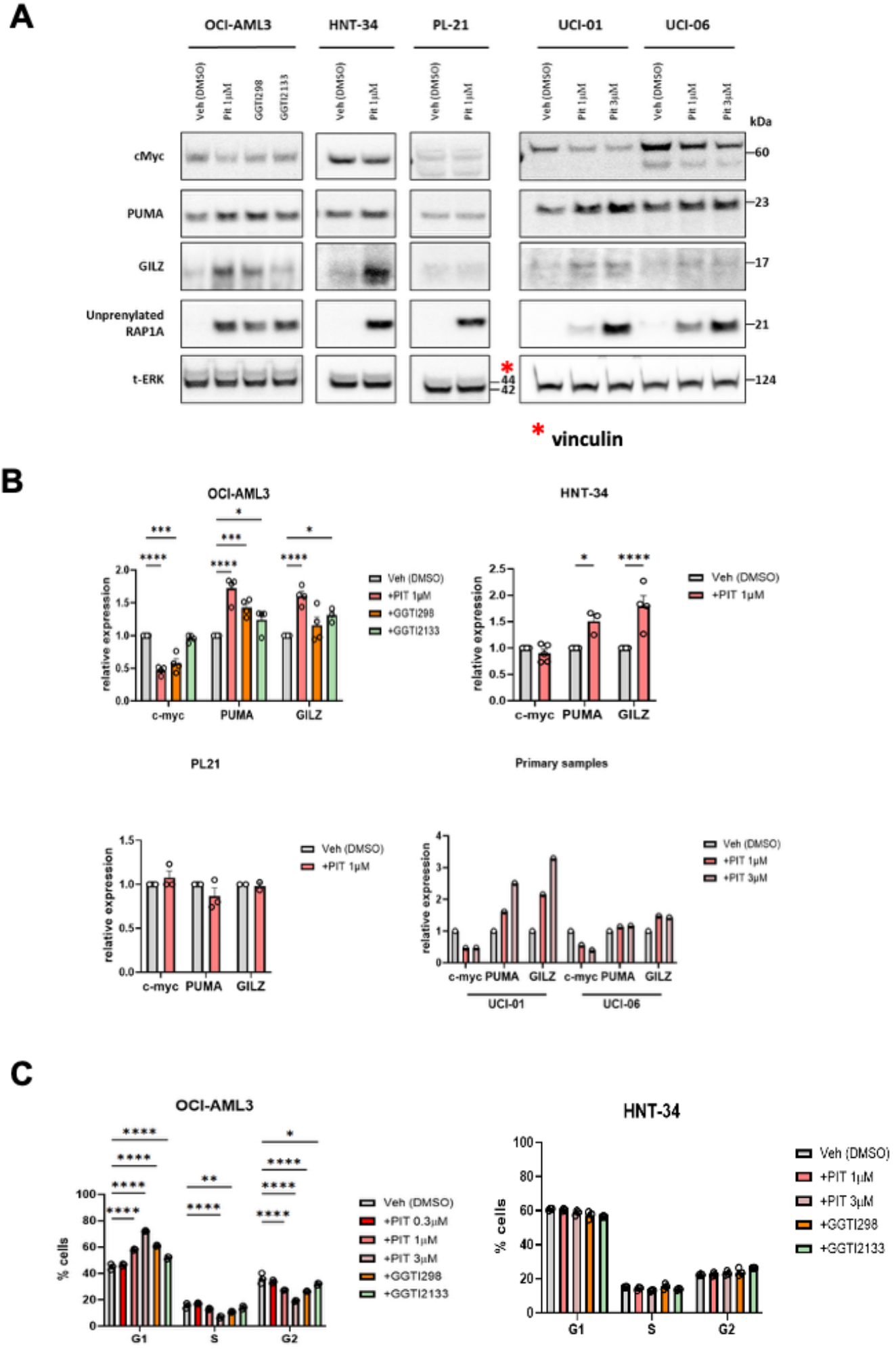
A
OCI-AML3
HNT-34
PL-21
UCI-01
UCI-06
Veh (DMSO)
Pit 1µM
GGTI298
GGTI2133
Pit 3µM
kDa
cMyc
PUMA
GILZ
Unprenylated RAP1A
t-ERK
60
23
17
21
44
42
124
* vinculin
B
OCI-AML3
HNT-34
PL21
Primary samples
relative expression
c-myc
PUMA
GILZ
Veh (DMSO)
+PIT 1µM
+GGTI298
+GGTI2133
+PIT 3µM
UCI-01
UCI-06
C
OCI-AML3
HNT-34
% cells
G1
S
G2
+PIT 0.3µM

Figure 5

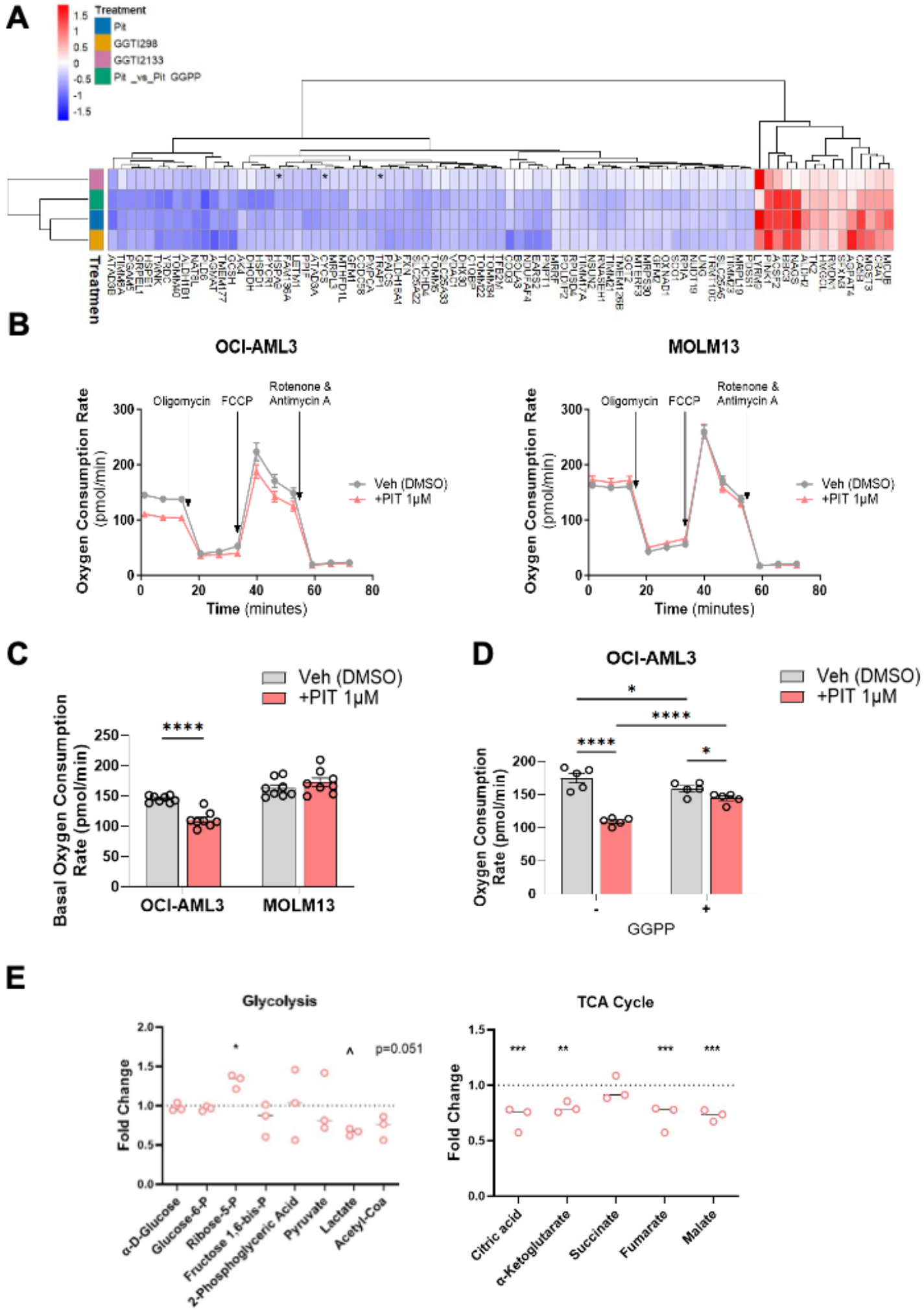
A
Treatment
Pit
GGTI298
GGTI2133
Pit _vs_Pit GGPP
B
OCI-AML3
MOLM13
Oligomycin
FCCP
Rotenone & Antimycin A
Oxygen Consumption Rate (pmol/min)
Time (minutes)
Veh (DMSO)
+PIT 1μM
C
Basal Oxygen Consumption Rate (pmol/min)
OCI-AML3
MOLM13
D
Oxygen Consumption Rate (pmol/min)
GGPP
E
Glycolysis
TCA Cycle
Fold Change
p=0.051
α-D-Glucose
Glucose-6-P
Ribose-5-P
Fructose 1,6-bis-P
2-Phosphoglyceric Acid
Pyruvate
Lactate
Acetyl-Coa
Citric acid
α-Ketoglutarate
Succinate
Fumarate
Malate

Figure 6

Table 1

Characteristics of different AML cell lines

AML Cell Line	Molecular Subtype	Origin	DNMT3A	FLT3	TP53	NPM1	Key Fusions	Notes
OCI-AML3	M4		R882		WT	mutation type A		Established from the peripheral blood of a 57-year-old man with M4.
HNT34	M4				unkown		BCR-ABL1	Established from the peripheral blood of a 47-year-old woman where the AML was transformed from MDS.
MOLM13	M5a, relapse	sAML		FLT3-ITD	WT		KMT2A-MLLT3	Established from the peripheral blood of a 20-year-old man with M5a at the time of relapse after an initial myelodysplastic syndrome
MOLM14	M5a, relapse	sAML		FLT3-ITD	WT		KMT2A-MLLT3	Established from the peripheral blood of a 20-year-old man with M5a at the time of relapse after an initial myelodysplastic syndrome
MV4.11	M5			FLT3-ITD	WT		KMT2A-AFF1	Established from the blast cells of a 10-year-old male with biphenotypic B myelomonocytic leukemia. Carries t(4;11) (q21;q23), typically observed in biphenotypic congenital leukemias.
OCI-M1					unkown			
PL21	M3	de novo			WT/P36fs			

Table S2

Characteristics of primary AML samples

Sample	Age	Sex	Disease	Disease Status	Molecular Cytogenetics	Treatment History
UCI-01	78	M	AML	New Diagnosis	46,XY,+19(3)/46,XY,add(19)(P13)(3)/46,XY(14)	No prior treatment
UCI-02	76	M	AML arising from MDS	New Diagnosis	44-45, XY, add (1) (p36.3), add (3) (P13), -4, add(5)(q11.2),-7 (q22),+8del(9) (q32),-10, add(17) (P11.2),-20,+2-3mar(cp16)	Azacitidine followed by Decitabine for MDS prior to AML diagnosis
UCI-03	59	F	AML	Relapse	FLT3 ITD, NPM1 XX	Idarubicin/Cytarabine.
UCI-04	61	F	AML M5	New Diagnosis	NPM1 mutant XX	No prior treatment
UCI-06	26	F	AML	New Diagnosis	CEBPA mutant (p.Asp301_Leu315dup) KIT mutant (p.Asp816His;) XX	No prior treatment
UCI-07	74	M	AML	New Diagnosis	NPM1 mutant (p.Trp288CysfsTer12) FLT3-ITD (ITD Size: 107bp) XY	No prior treatment
UCI-08	50	F	AML	New Diagnosis	NPM1 (p.Trp288CysfsTer12) DNMT3A mutant (p.Arg882His) XX	No prior treatment
UCI-09	83	F	AML	New Diagnosis	NPM1 (p.Trp288CysfsTer12) FLT3-ITD (ITD Size: 26pb) XX	No prior treatment
UCI-10	41	F	AML	New Diagnosis	FLT3-ITD	No prior treatment
UCI-11	77	M	MDS/MPN transformed to AML	Transformation to AML	complex karyotype, monosomy 7, deletion of 12p,and isochromosome 17q	Hydrea for MDS/MPN prior to AML diagnosis
UCI-12	43	F	AML	Relapse	FLT3-ITD	Idarubicin/Cytarabine
LBV-03	80	M	AML	New Diagnosis	Trysomy 8 / duplication of 8q22 and gain of KMT2A	No prior treatment
UPENN-01			AML	New Diagnosis	TP53 frameshift mutation with der(17)t(11;17)	
TUPENN-02			AML	New Diagnosis	TP53 missense Y220C, CBL, NPM1, TET2 mutations, VUS EGR2	